Supporting Information

Tumor Microenvironment-Regulated Nanoplatform for Enhanced Chemotherapy, Cuproptosis and Nonferrous Ferroptosis Combined Cancer Therapy

Xiangyu Meng,[a,b,c] Lu Tian,*[a,c] Jingmei Zhang,[e] Jiaoyu Wang,[a,b,c] Xuewei Cao, [d,b,c] Zunfu Hu,[c] Yunqiang Sun,[a] Zhichao Dai,*[a,c] Xiuwen Zheng*[b,c]

[a]College of Chemistry and Chemical Engineering, Linyi University, Linyi 276000, P. R. China

[b]Qilu Normal University, Jinan 250000, P. R. China

[c]Key Laboratory of Advanced Biomaterials and Nanomedicine in Universities of Shandong, Linyi University, Linyi 276000, P. R. China

[d]College of Medicine, Linyi University, Linyi 276000, P. R. China

[e]School of Chemical Engineering, Hebei Normal University of Science and Technology, Qinhuangdao 066000, P. R. China

*Corresponding authors.

Tel./Fax: +86-539-7258629

E-mail: daizhichao@lyu.edu.cn (Z. D.); tianlu1021@126.com (L. T.); zhengxiuwen@lyu.edu.cn (X. Z.).

Experimental section

Materials

$Ce(NO_3)_3 \cdot 6H_2O$, ethylene glycol, propanoic acid, supplied by aladdin Company. Hyaluronic acid (HA) was obtained from Freda Biotechnology (Shandong, China). 3,3',5,5'-tetramethylbenzidine (TMB) were bought from Sigma-Aldrich. Hydrochloride (DOX·HCl) and inhibitor of glutathione peroxidase 4 (GPX4) (RSL3) was purchased from aladdin Company. Ltd. 2,7-dichlorodihydrofluorescein diacetate (DCFH-DA), Cell Counting Kit-8 (CCK8), Hoechst 33342, probes were obtained from Beyotime Biotechnology. C11-BODIPY581/591 were purchased from Thermo-Fisher. HRP-labeled goat anti-rabbit IgG (H+L) and ECL western blotting system were obtained from Beyotime Biotechnology. Alexa Fluor 555-labeled goat anti-Rabbit IgG (H+L), GPX4 (DF6701), HIF-1α (D1S7W) Rabbit mAb were purchased from Affinity Biosciences.

Characterizations.

The morphology and sizes of the samples were observed on a transmission electron microscopy JEM-2100. Zeta potential and hydrodynamic sizes of the samples were measured on Malvern Zeta Sizer-Nano Z instrument. UV-vis absorption spectrum was measured on a UV-Vis spectrophotometer. The concentrations of Ce were measured by inductively coupled plasma mass spectrometry. X-ray diffraction (XRD) analysis of CeO_2 were measured by D8-Advance diffractometer (Bruker, Germany). Fourier transform infrared (FT-IR) spectra of HA, CCDR and CCDRH were recorded by an FT-IR spectrometer (Nicolet 6700, ThermoFisher Scientific). X-ray photoelectron spectra (XPS) of CCDRH was examined using a Thermo Scientific EscaLab 250Xi instrument (ThermoFisher Scientific).

Supporting methods

Detection of ·OH.

The generation of •OH was determined by chromogenic reaction using 3,3',5,5'-tetramethylbenzidine (TMB) as the agent. The nanoparticles were added to the PBS solution (pH 5.8 and pH 7.4) containing TMB (0.8 mM) and stirred for 5 min. The absorption spectrum of mixture was recorded by UV-Vis spectrometer.

In vitro detection of O_2.

CCDRH (5 mg) was dispersed in deoxygenated PBS buffer (10 mL) at pH 5.8, and the O_2 concentration at different time points was monitored using a portable dissolved oxygen meter. As a control, the O_2 changes of PBS buffer at pH 5.8 (10 mL) was measured under the same condition.

In vitro detection of H_2O_2.

The H_2O_2 generation of CCDRH was investigated via the titanium sulfate colorimetric method. In brief, 100 μL of $Ti(SO_4)_2$ solution (100 mL of $Ti(SO_4)_2$ solution containing 2.7 mL of $Ti(SO_4)_2$ (24%) and 16.7 mL of H_2SO_4) was added into PBS (1.9 mL, pH 5.8) solution containing different concentration of CCDRH, and the UV-Vis absorption of the solution at 405 nm was recorded.

Cytotoxicity

The in vitro cytotoxicity of nanoparticles toward 4T1 cells was evaluated using the CCK-8 assay. 4T1 cells were seeded in a 96-well plate at a density of 5×10^3 cells per well and incubated for 24 h at 37 ℃ with 5 % CO_2. Subsequently, the nanoparticles including CH, CCH, CCDH, CCRH and CCDRH with different concentrations were added to the cells and incubated at 37 ℃ with 5 % CO_2 for 24 h, respectively. Subsequently, 10 μL CCK-8 solution was added to each well of the 96-well plate. After incubated for 3 h, the optical density (OD) of each well was measured at 450 nm.

Cellular LPO detection

The intracellular LPO level in cells was assessed with BODIPY™581/591-C11. 4T1 cells were seeded in confocal dishes for 24 h and treated with different nanoparticles (CH, CCH, CCDH, CCRH and CCDRH). After incubation for 12 h, the cells were washed with medium and stained with BODIPY581/591-C11 (5 μM) for 20 min. Finally, the cells were observed by CLSM.

Immunofluorescence staining of HIF-1*α*.

4T1 cells were seeded in confocal culture dishes and incubated for 12 h. Then cells were treated with PBS, CH, DOX, CCDH and CCDRH for another 12 h, respectively. Afterwards, the cells were fixed with 4% paraformaldehyde for 15 min and washed with PBS for three times. The sample was blocked with immunofluorescence blocking buffer for 1 h at room

temperature. Then, the primary HIF-1α antibody was added and incubated for another 1 h. The cells were washed for three times with PBS and incubated with the secondary Alexa Fluor 555-conjugated goat anti-rabbit IgG H&L antibody for 1 h. The sample was washed for three times with PBS and stained with DAPI for 15 min. Finally, the cells were washed and then imaged by CLSM. In addition, Immunofluorescence Staining of GPX4, DLAT, FDX1 and LIAS were performed with similar procedures.

Western blotting analysis of GPX4.

4T1 cells were seeded into 6-well plates at a density of 5×10^5 cells per well. After culture for 12 h, PBS, CH, CCH, CCDH, CCRH and CCDRH were added into the medium, respectively. After incubation for 24 h, the cells were rinsed twice carefully with PBS. Then 4T1 cells were collected and lysed in a universal lysis buffer. A BCA Protein Assay Kit was firstly used to quantify the total protein, and then the total protein concentration was adjusted to make a consistent concentration among every groups. The target proteins were separated by SDS-PAGE and transferred to PVDF membranes. After 1 h of blocking with 5 % nonfat dry milk buffer, proteins on the polyvinylidene difluoride membrane were incubated with GPX4 primary antibody (1:1000 diluted) overnight at 4°C, followed by secondary antibody incubation for 1 h at room temperature. Anti-β-Actin (1:1000 diluted) were used as a loading control. Corresponding secondary antibodies were further incubated to detect enhanced chemiluminescence. All antibodies mentioned above are rabbit antibodies.

GSH depletion assay.

Intracellular GSH concentration was determined by the GSH and GSSG assay kits. 4T1 cells were incubated with different nanomaterials for 24 h. Thereafter, the cell samples were collected by digestion and intracellular GSH levels were detected using the GSH assay kit.

In vitro hemolysis test.

2 mL of fresh blood were obtained from the mouse through centrifuged at 3000 rpm for 5 min. The supernatant was discarded, and the erythrocytes left in the bottom of the tube were washed five times with PBS. Then the 2% (v/v) red blood cell suspension in saline buffer was prepared. After incubated with CCDRH NPs (0, 20, 40, 60, 80, 100 and 120 μg/mL) at 37 ℃ for 12 h, the samples were centrifuged and the UV-vis absorbance of the supernatants at 540 nm was measured.

In vivo fluorescence imaging

The mice were intravenously injected with CCDRH-Cy5 NPs and the fluorescence images of mice at predetermined time intervals (1, 4, 12, 16 and 24 h post-injection) were obtained using the animal living body fluorescent imaging instrument. After 12 h post injection, the mice were sacrificed and the tumor and major organ tissue (such as heart, liver, spleen, lung and kidney) were collected for ex vivo fluorescence imaging.

In vivo tumor inhibition.

When the tumor volume of 4T1 cell-bearing mice reached ~80 mm^3, the mice were divided randomly into 6 groups. All groups were intravenously administrated into PBS, CH, CCH, CCDH, CCRH and CCDRH (10 mg/kg) on the day of 1, 3, 6, 9, 12 and 15. During the treatments, all mice's body weights and tumor volumes were recorded every 3 days. The tumor volumes were calculated through the following formula: $V = 0.5 \times L \times W^2$ (L: the longest diameter of the tumor, W: the shortest diameter of the tumor). After 15 days of treatment, all mice were sacrificed and the tumor and major organs were harvested for further histological analysis.

Statistical analysis

All experiments were performed five times, and the statistical analysis results are shown as mean ± standard deviation (SD). The student's t-tests determined statistical comparisons between experimental groups.

Supporting Figures

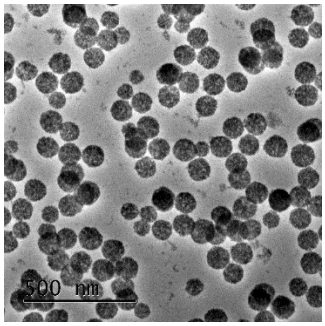

Figure S1. Transmission electron microscopy (TEM) image of CeO_2.

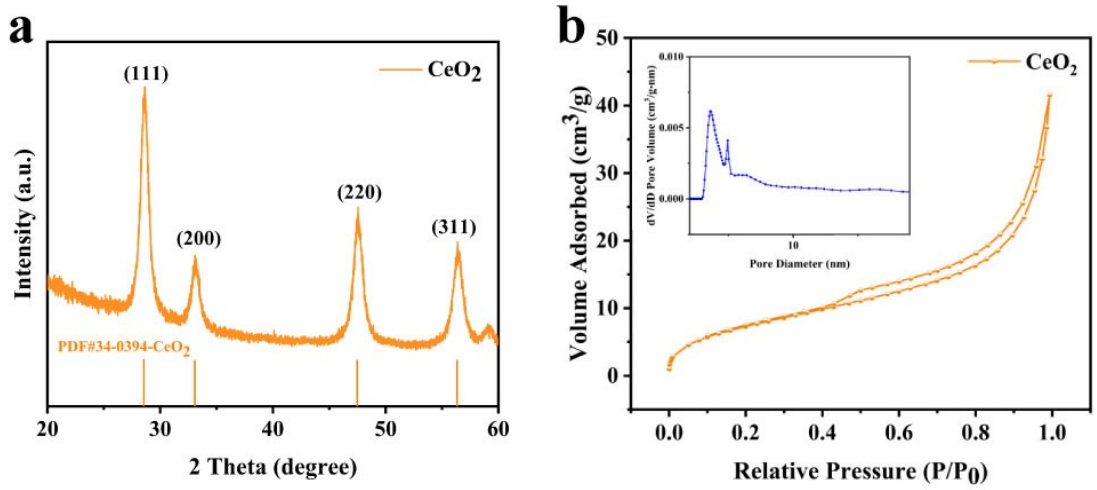

Figure S2. (a) X-ray diffraction image of CeO_2; (b) N_2 adsorption–desorption isotherms and pore-size distribution of CeO_2.

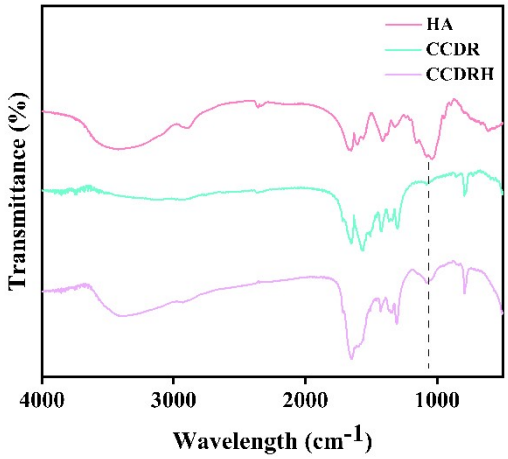

Figure S3. The FTIR spectra of HA, CCDR and CCDRH.

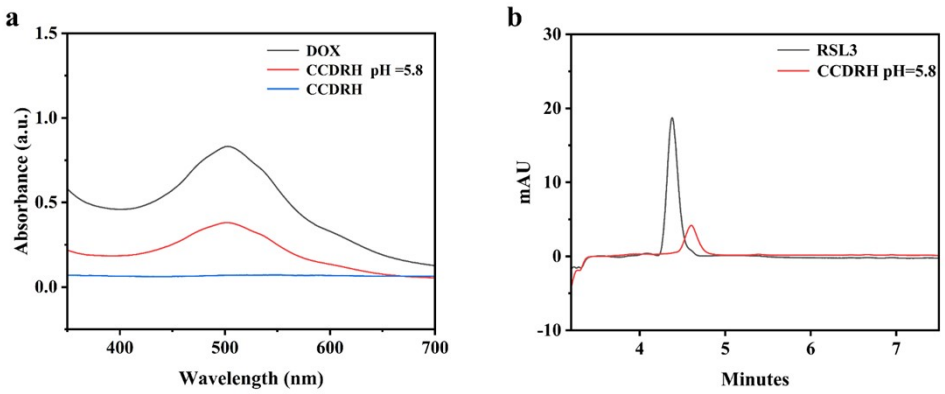

Figure S4. (a) UV-vis absorbance spectra of DOX and CCDRH in PBS of pH 5.8; (b) HPLC of RSL3 and CCDRH in PBS of pH 5.8.

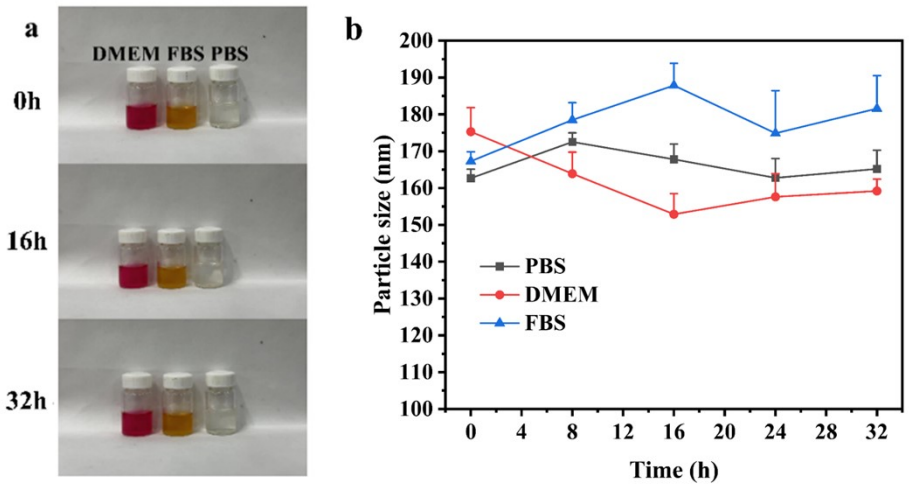

Figure S5. (a) The stability of CCDRH in PBS, DMEM and fetal bovine serum (FBS) after 32 h; (b) The changes of hydrodynamic size of CCDRH in PBS, FBS and DMEM within 32 h.

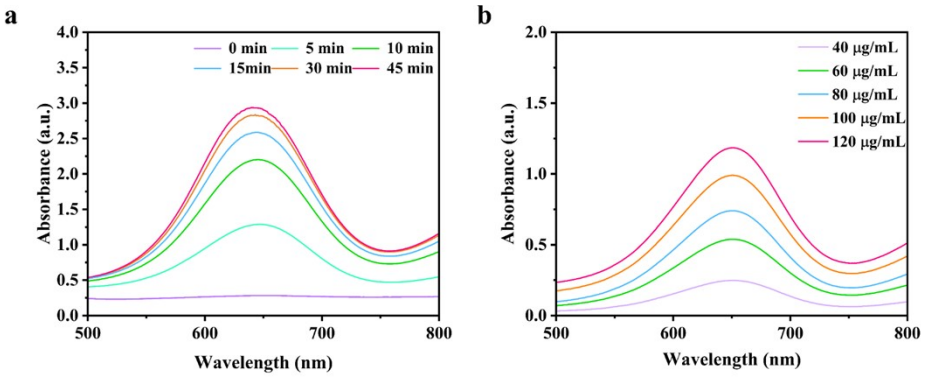

Figure S6. (a) UV-vis absorbance variations of TMB at various reaction time in the presence of CCDRH; (b) UV-vis absorbance variations of TMB with different CCDRH contents.

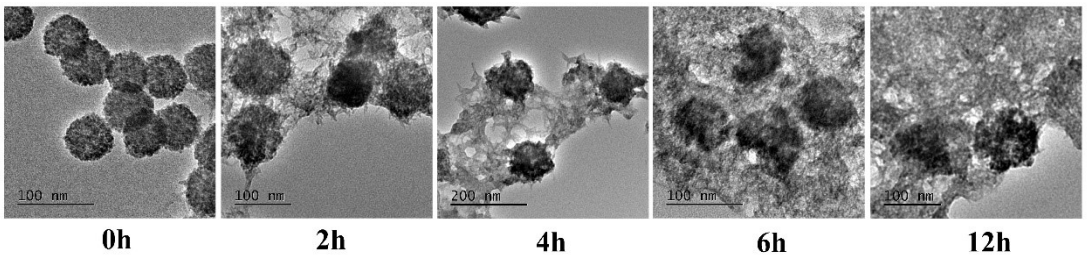

Figure S7. TEM images of CCDRH at PBS solution of pH 5.8.

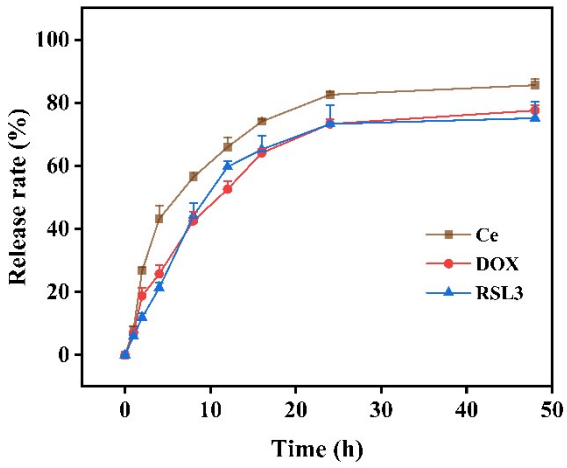

Figure S8. Time-dependent release behavior of CCDRH at PBS solution of pH 5.8.

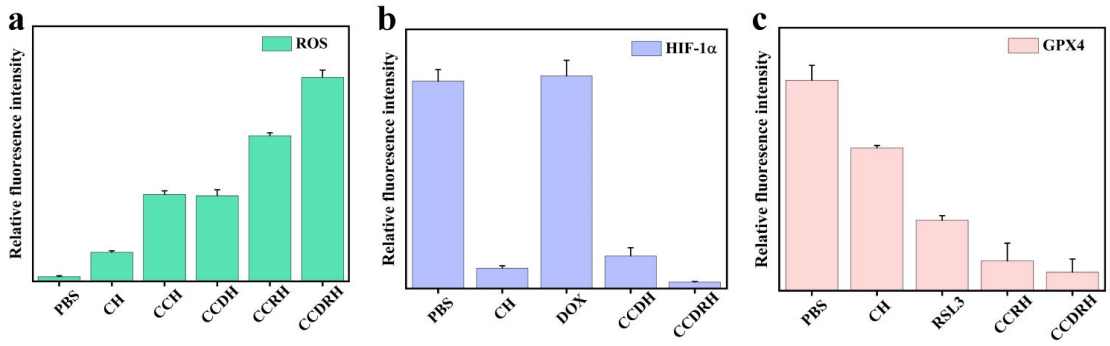

Figure S9. The relative mean fluorescence intensities of ROS (a), HIF-1α (b) and GPX4 (c).

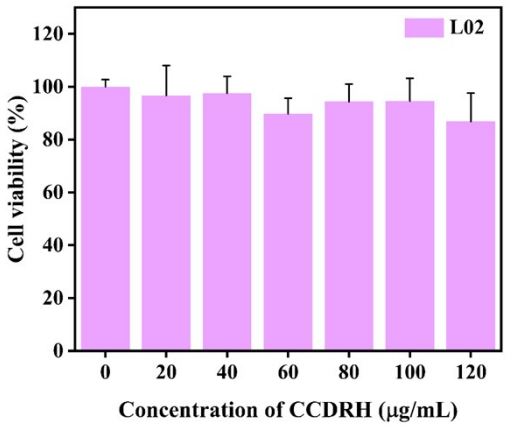

Figure S10. The variation of L02 cells viability after treatment with different contents of CCDRH for 24h. Data are expressed as means ± standard deviation (SD) (n = 3).

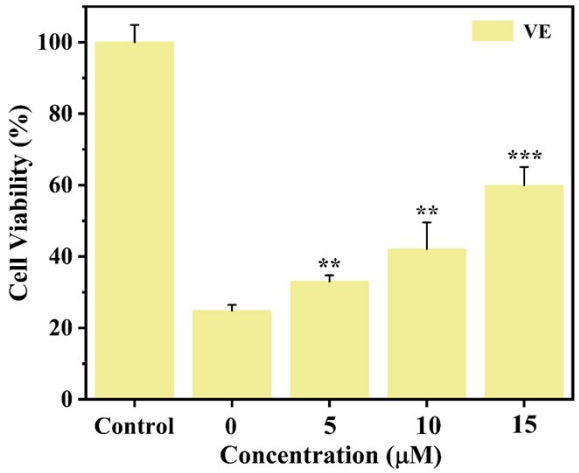

Figure S11. Viability of 4T1 cells after the addition of VE. Data represent means ± SD (n =3). (Data were analyzed with ordinary one-way ANOVA by Tukey means comparison method. *p < 0.05, **p < 0.01 and ***p < 0.001).

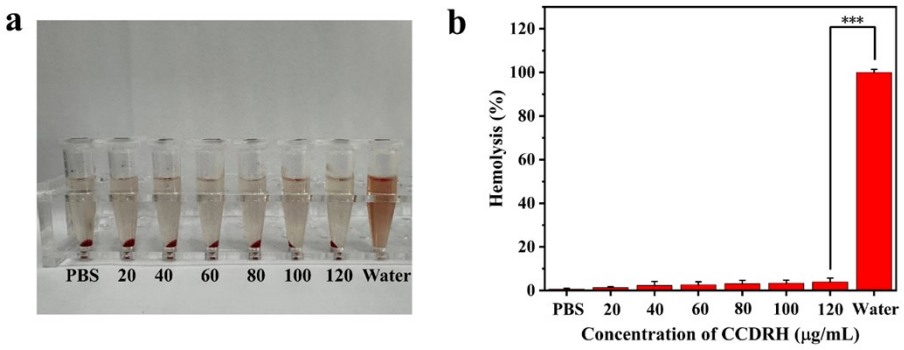

Figure S12. (a) Photograph of RBC suspensions after treatment with various concentrations of CCDRH. (b) Corresponding hemolysis rates of the RBC samples in (a). (Data were analyzed with ordinary one-way ANOVA by Tukey means comparison method. *$p < 0.05$, **$p < 0.01$ and ***$p < 0.001$).

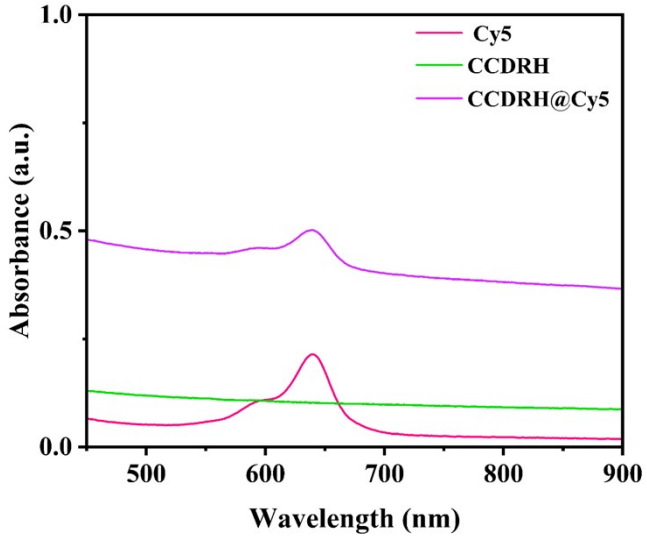

Figure S13. UV-vis absorption spectra of Cy5, CCDRH and CCDRH@Cy5.

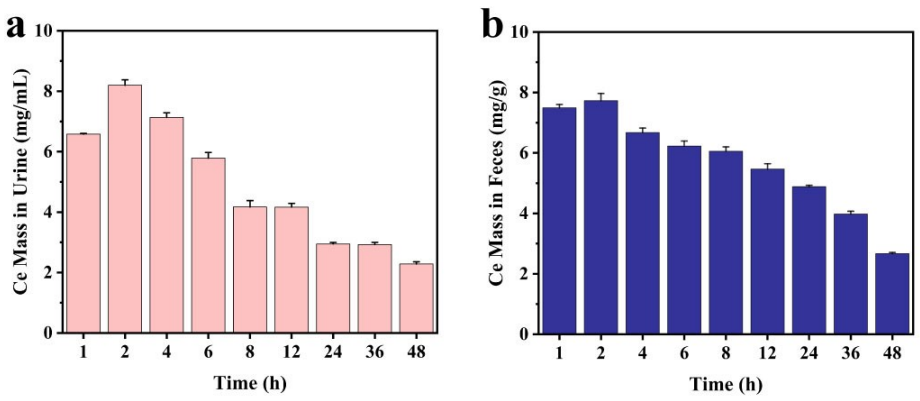

Figure S14. Ce content in the urine and feces after the injection of CCDRH via the tail vein at different time intervals.

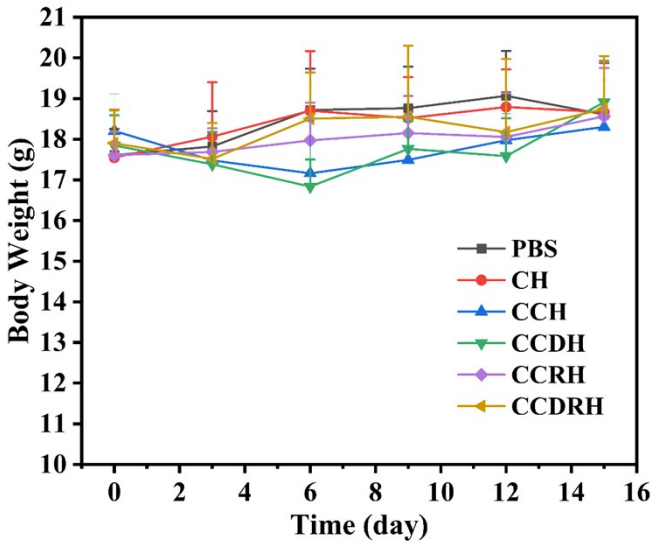

Figure S15. Variation of mice body weight in various groups. Data represent means ± SD (n =5).

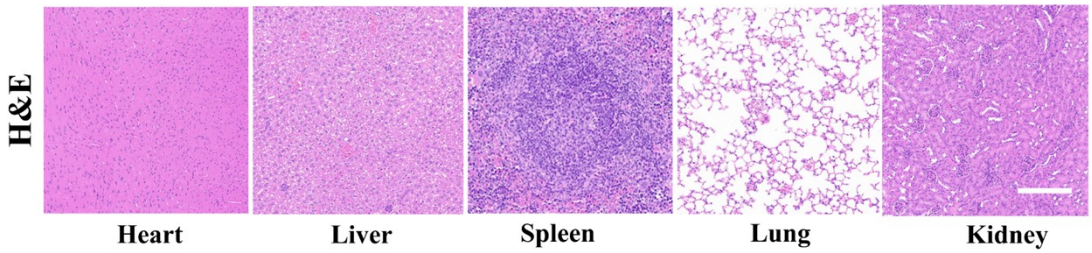

Figure S16. H&E stained images of major organs derived from the mice after treatment with CCDRH for 15 days (scale bar = 100 μm).